JOURNAL OF MATERIALS SCIENCE **36** (2001) 5519–5527

Properties of sol-gel derived strontium barium niobate ceramics and the effect of V_2O_5 additive

A. Y. ORAL, M. L. MECARTNEY
University of California, Irvine, Department of Chemical and Biochemical Engineering and Materials Science, Irvine, CA 92697-2575, USA
E-mail: martham@uci.edu

Strontium barium niobate, $Sr_xBa_{1-x}Nb_2O_6$, (SBN) ceramics with a range of Sr/Ba ratios were fabricated using a solution chemistry approach with alkoxides dissolved in acetic acid. Powders obtained from dried gels were calcined at 800°C for three hours, a heat treatment that produced fully crystalline powders. After preparing bulk ceramics from these powders by sintering at 1200°C for 1–24 hours, the tetragonal tungsten bronze (TTB) phase was present in all compositions between $0 \leq x \leq 1$, although not predicted by the phase diagram for $BaNb_2O_6$ and $SrNb_2O_6$. Vanadium pentoxide (V_2O_5) additions increased the densification, the amount of tungsten bronze phase, and the dielectric constant for all compositions except for $Sr_{0.65}Ba_{0.35}Nb_2O_6$ (SBN65) ceramics.

1. Introduction

$Sr_xBa_{1-x}Nb_2O_6$ (SBN) ceramics are potential materials for pyroelectric infrared detectors, piezoelectrics, electro-optics, and photorefractive optics [1]. Although there have been a remarkable progress in growing high quality single crystals of SBN, cost is still a limiting factor for their application [2, 3]. In addition, it is difficult to produce single crystals except for the congruent composition (SBN60) due to redistribution of excess components at the growing interface [4]. Polycrystalline ceramics have the advantage of easy fabrication of large sizes and complex shapes, and a stress resistance [2, 5, 6].

SBN ceramics have been produced with a high density and fairly good electrical properties using conventional ceramic fabrication techniques [2, 3, 5–9]. In general, the dielectric, piezoelectric and pyroelectric properties of SBN ceramics exhibit smaller coefficients than those observed in single crystals, probably due to a lower degree of orientation [6]. Conventional processing techniques for SBN ceramics use high sintering temperatures ($T_s > 1300$) for fabrication [3, 5–9]. Moreover, very fine powders ($d_p < 1$ μm), often produced by ball milling, are required to decrease the required diffusion range for sintering and achieve high densities. In general, high sintering temperatures and fine powder preparation result in a major increase in the cost of the production. Furthermore, the probability of contamination increases, especially when wet ball milling is used.

Additives are commonly used in the fabrication of ceramics to aid in densification, control grain growth, and enhance desired properties. Vanadium pentoxide (V_2O_5), which melts at 690°C, is a suitable sintering additive since the liquid phase formed at sintering temperatures accelerates the sintering and densification process. Nishiwaki *et al*. [9] used V_2O_5 as a densification agent for SBN30 powders and obtained 96% of the theoretical density at the sintering temperature of 1300°C after 4 hours versus 65% density without V_2O_5. They also found that V_2O_5 additions eliminate the relaxor behavior of SBN30 ceramics and suggested that V^{+5} cations were intercorporated into small C-sites and caused a substantial ordering in the distribution of Sr^{+2} and Ba^{+2} cations. The highest dielectric constant for SBN30 ceramics was measured in samples with an addition of 1 wt% V_2O_5.

In present work, we report on the fabrication of SBN ceramics produced from the powders obtained by solution chemistry processing and compare the effect of V_2O_5 additions to a range of SBN compositions from $SrNb_2O_6$ to $BaNb_2O_6$.

2. Experimental procedure

A flow diagram of the experimental procedure is given in Fig. 1. The sols were prepared by dissolving Ba-isopropoxide and Sr-isopropoxide in acetic acid and mixing the resulting solution with Nb-ethoxide. The final solution, with a concentration of 0.36 M, was clear light brown without any observable particles. Gelation started several hours after exposing the solution to air. A transparent solid xerogel obtained after 2 days of air-drying. The xerogel was calcinated at 800°C for 3 hours to burn off organics and to crystallize the material, and then crushed and sieved to a particle size less than 36 μm. At this point, 1 wt% V_2O_5 powder was mixed in with certain samples. The fine powder was compacted into rectangular prisms using a cold isostatic press (CIP) with a pressure of 50,000 psi. Finally,

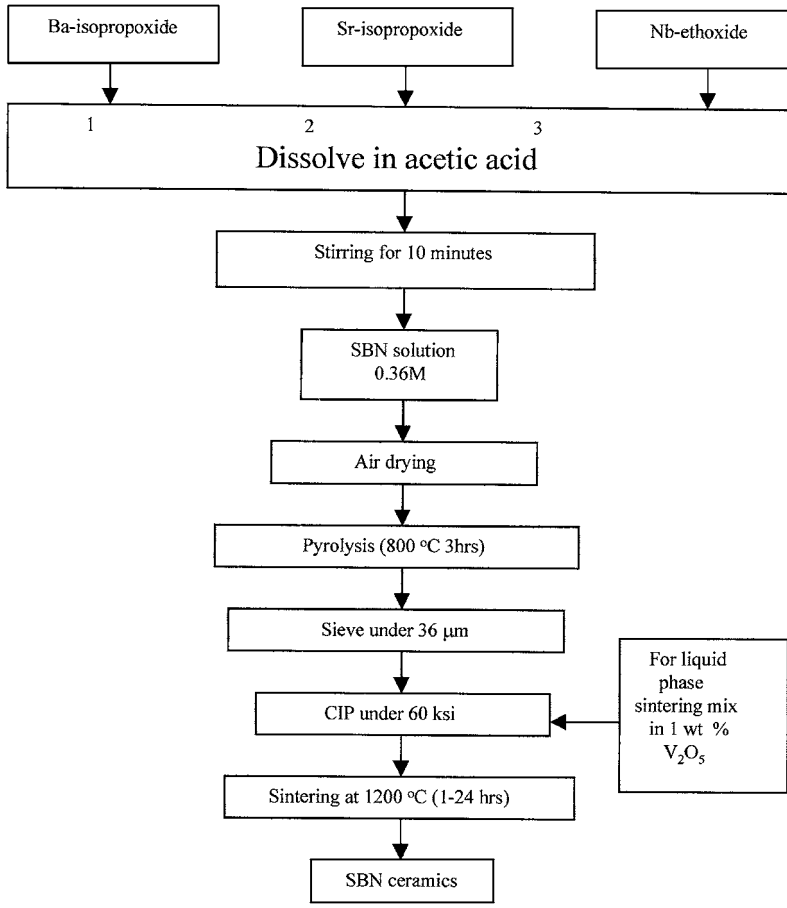

Figure 1 Flowchart of SBN ceramic production by modified sol-gel technique.

the green body was sintered at 1200°C for 1–24 hours to produce dense ceramics.

Alcohol based sols are difficult to prepare due to their high sensitivity to the moisture in air, and short shelf life [10]. The sol preparation method using acetic acid as a main solvent eliminates these problems, since acetic acid is a suitable chelating agent making the sols less susceptible to fast hydrolysis [11].

The crystallization behavior and the surface topology of the ceramics were analyzed by Siemens D5000 X-ray diffraction (XRD), and by Philips XL 30 FEG scanning electron microscope (SEM).

3. Results and discussion

3.1. Crystallization behavior

Four different crystalline phases form throughout the solid solution ($0 \leq x \leq 1$) after the calcination of sols at 800°C. Orthorhombic $BaNb_2O_6$ is identified near the $BaNb_2O_6$ end as predicted from the phase diagram (Fig. 2a). An unexpected crystal structure, with d-spacings and intensities similar to hexagonal (pseudo-orthorhombic) $BaNb_2O_6$, forms for compounds with a low Sr content (Fig. 2b) along with some of the tetragonal tungsten bronze phase of SBN. Tetragonal tungsten bronze SBN exists as a single phase only in a narrow composition range around $x = 0.65$ (Fig. 2c). Near the $SrNb_2O_6$ end ($0.85 \leq x$), the orthorhombic $SrNb_2O_6$ structure (isostructural with $CaTa_2O_6$) is dominant, as expected from the equilibrium phase diagram (Fig. 2d).

The crystallization behavior of sol-gel derived SBN powders is considerably different than for powders produced by conventional processing techniques. This solution chemistry technique makes it possible to obtain 100% reacted and crystalline SBN at temperatures as low as 575°C in contrast to the conventional techniques requiring temperatures between 1000–1480°C [2, 5, 7, 9]. In conventional techniques, the required calcination temperature increases as the Sr content of the solid solution increases due to the increase in lattice distortion arising from smaller Sr^{+2} ions in the large A2 sites [12]. In this solution chemistry system, a single tetragonal tungsten bronze phase can be obtained near $x = 0.65$ after calcination at 800°C (Fig. 2). The reason for this formation temperature reduction should be the increasing instability of the hexagonal (pseudo-orthorhombic) $BaNb_2O_6$ structure and the instability of the single size (large) interstitial sites with increasing concentration of small Sr ions. When two different cations with considerable size differences are present in equal numbers, the tungsten bronze structure with two different size of interstitial sites becomes more stable due to less strain in the structure.

XRD studies show that the solid solution tungsten bronze region is extended when these powders, produced by solution chemistry approach, are sintered as bulk ceramics at 1200°C (Fig. 3). The tungsten bronze phase at least partially forms in all compositions between $0 \leq x \leq 1$ after sintering at 1200°C for samples with and without V_2O_5 additions (Figs 3 and 4).

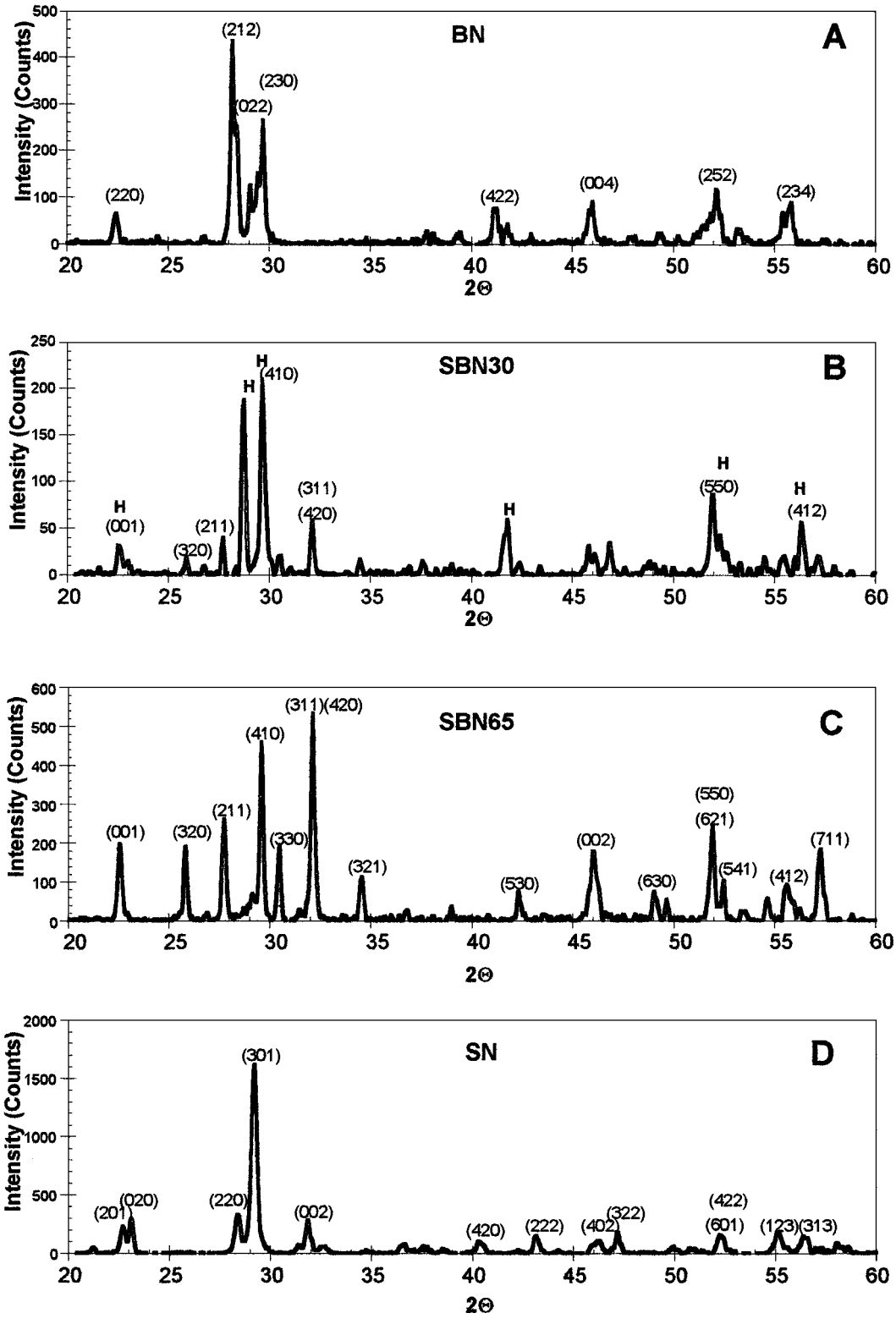

Figure 2 XRD patterns of dried sols calcined at 800°C for 3 hours. (a) Orthorhombic phase of $BaNb_2O_6$ in BN; (b) Hexagonal/pseudo-orthorhombic phase (H) and tetragonal tungsten bronze phase in SBN30; (c) Tetragonal tungsten bronze phase in SBN65; (d) Orthorhombic $BaNb_2O_6$ phase in SN.

In bulk samples sintered at 1200°C, $BaNb_2O_6$ mainly crystallizes as the tungsten bronze structure along with an unknown phase (too many overlapping peaks to clearly identify the compound) and V_2O_5 additions significantly increase the amount of the tungsten bronze phase and minimize the amount of the unknown phase (Figs 3a and 4a). There is no evidence of any orthorhombic $BaNb_2O_6$ that had formed after the calcination at 800°C and would be expected by the $BaNb_2O_6$-$SrNb_2O_6$ phase diagram. This barium metaniobate phase may be oxygen deficient $BaNb_2O_5$ formed after annealing at 1200°C without any O_2 flow, producing the tetragonal tungsten bronze structure instead of the orthorhombic phase [13]. XRD results obtained from SBN30, annealed at 1200°C, also show the presence of the tungsten bronze phase (Fig. 3b). The same composition mainly yielded the unexpected, presumably hexagonal (pseudo-orthorhombic) phase after the calcination at 800°C (Fig. 2b). The transformation of hexagonal (pseudo-orthorhombic) phase to the tetragonal

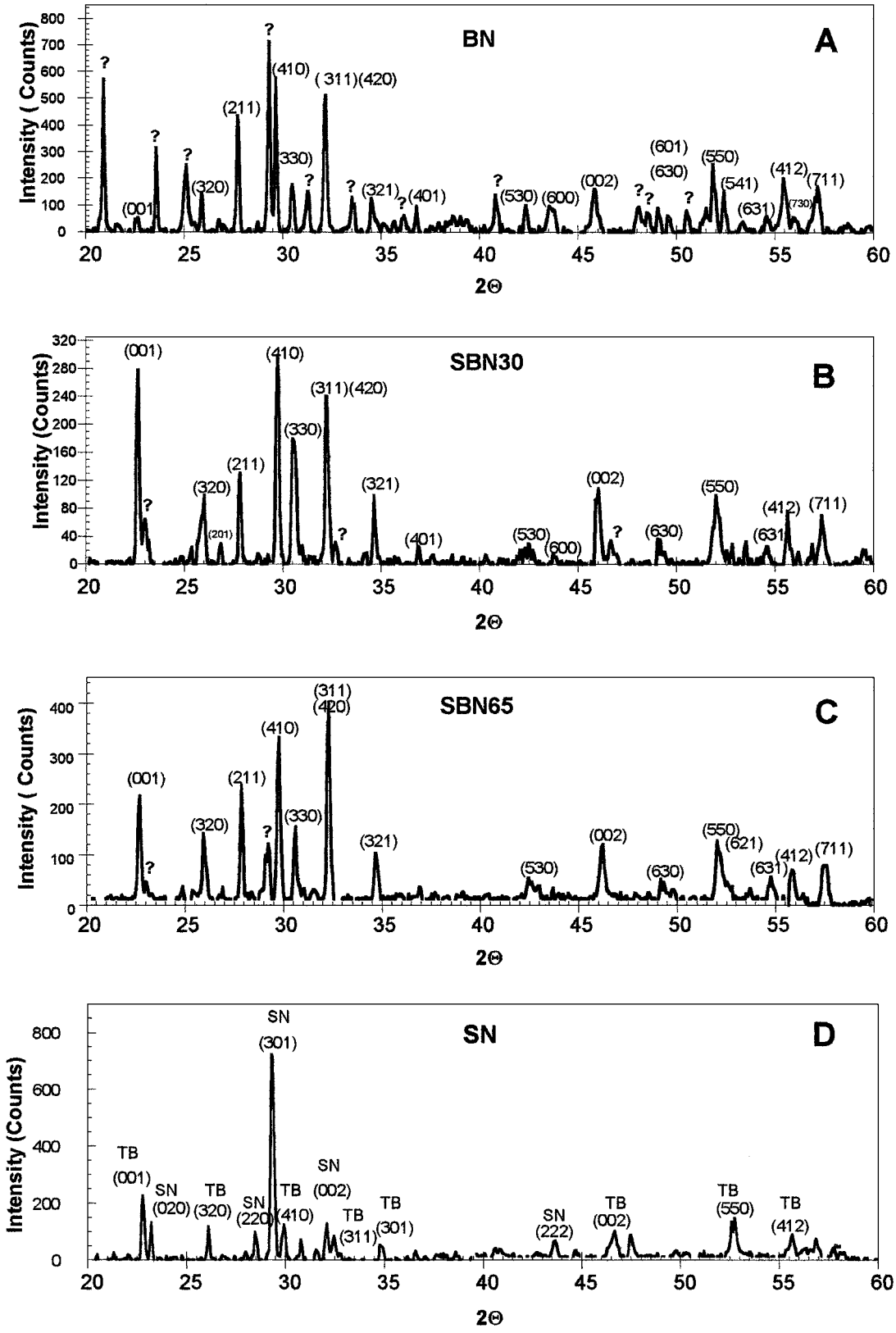

Figure 3 XRD patterns of bulk ceramic sintered at 1200°C for 24 hours. (a) Tetragonal tungsten bronze and unknown phase in BN; (b) Tetragonal tungsten bronze phase in SBN30; (c) Tetragonal tungsten bronze and unknown phase in SBN65; (d) Orthorhombic (SN) and tetragonal tungsten bronze (TB) phases in SN.

tungsten bronze suggests that the lower temperature pseudo-orthorhombic phase is metastable. Additions of V_2O_5 do not show any pronounced effect (Fig. 4b) on the crystal structure of SBN30 but do indicate texturing due to the different intensity ratios in the XRD pattern. For SBN65 ceramics sintered at 1200°C, the unknown phase is encountered in addition to the tungsten bronze phase (Fig. 3c). Since SBN65 powders had formed 100% tungsten bronze phase after the calcination at 800°C (Fig. 2c), this unknown phase must have developed during sintering at 1200°C. $SrNb_2O_6$ ceramics that were fully orthorhombic after calcination at 800°C, primarily crystallize after sintering at 1200°C as the orthorhombic ($CaTa_2Nb_6$) structure as expected

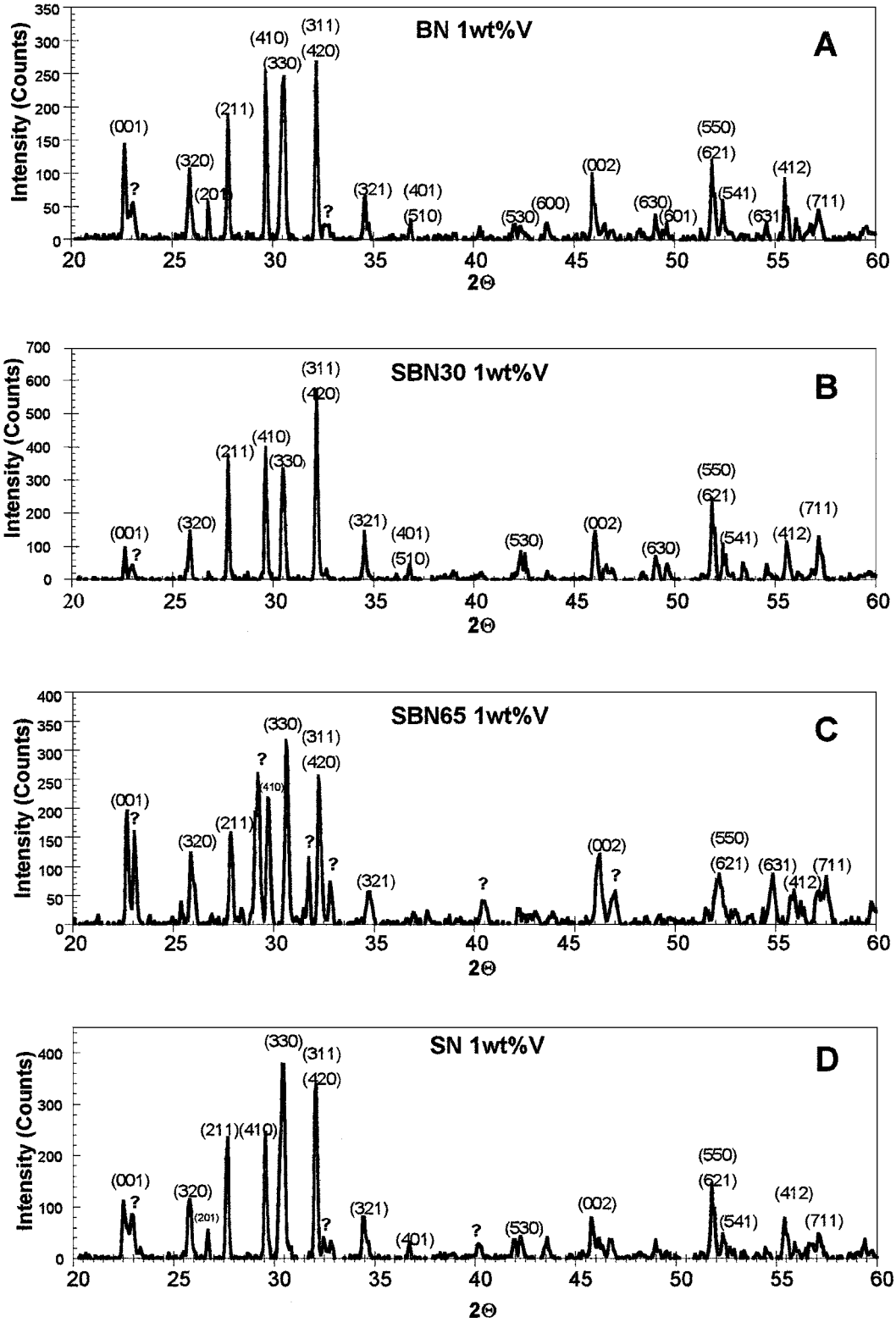

Figure 4 XRD patterns of ceramics with 1 wt% V_2O_5 sintered at 1200°C for 24 hours. (a) Tetragonal tungsten bronze phase in BN; (b) Tetragonal tungsten bronze phase in SBN30; (c) Tetragonal tungsten bronze and unknown phase in SBN65; (d) Tetragonal tungsten bronze phase in SN.

by the phase diagram, but some tungsten bronze structure is also present (Fig. 3d). The tungsten bronze structure is very unusual in $SrNb_2O_6$ compounds and has not been identified previously. Addition of 1 wt% V_2O_5 to $SrNb_2O_6$ produces a material with a dominant tetragonal bronze phase (Fig. 4d). Thus, V_2O_5 additions facilitate the formation of the tungsten bronze phase for all compositions except SBN65, in which V_2O_5 additions enhance the formation of an unknown phase (Fig. 4).

It should be noted that structures of both $SrNb_2O_6$ (SN) and $BaNb_2O_6$ (BN) are very sensitive to changes in the valance state of Nb [13]. Partial reduction of Nb causes orthorhombic SN to become a cubic perovskite. Barium niobium bronzes ($BaNb_2O_5$) that contain reduced states of niobium crystallize as the tetragonal tungsten bronze structure. Barium deficient compounds such as $3BaO^*5Nb_2O_5$ also form a distorted tetragonal bronze structure where the Nb-O bond is

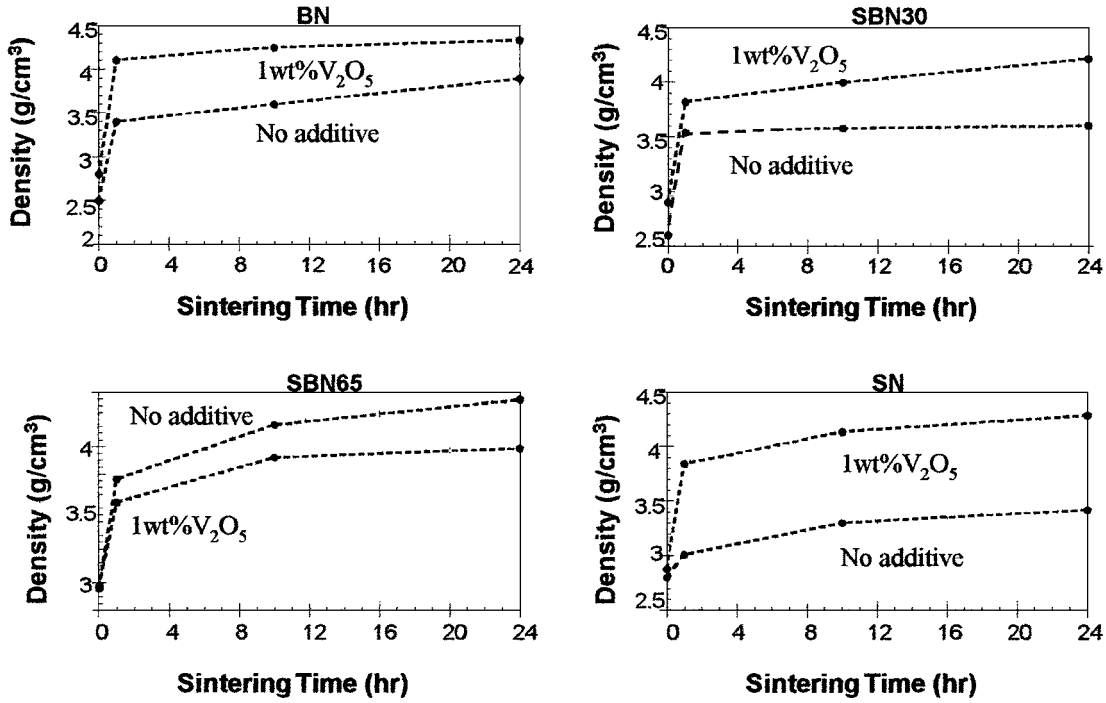

Figure 5 Variation of the density of SBN bulk ceramics versus sintering time at 1200°C.

lengthened and weakened by A2 site shrinkage [14]. The metastable hexagonal/psuedo-orthorhombic structure of $BaNb_2O_6$ is a transition between a tetragonal tungsten bronze and orthorhombic structure. The addition of the vanadium oxide could either reduce the niobium, making the tungsten bronze structure preferred, or structurally stabilize the tungsten bronze structure by minimizing strain energy.

There are two different arguments advanced about the effect of valance state of Nb on the crystal structure of SBN. Ballman and Brown [15] suggest that the primary requisite for the formation of tungsten bronze structure is that the niobium ion be reduced. They propose that SBN forms the tetragonal tungsten bronze structure because of a partial reduction of Nb by excess Sr^{+2} and Ba^{+2} and so the true formula of the structure is $(Sr^{+2}, Ba^{+2})(Nb^{+5}, Nb^{+4})_2O_6$. Neurgaonkar *et al.* [16] claim that if the oxygen partial pressure is sufficiently low, Nb^{+5} converts to the Nb^{+4} and prevents the formation of the tetragonal tungsten bronze phase formation. Ballman and Brown's argument, however, is in agreement with the observation that oxygen deficient $BaNb_2O_5$, with reduced states of Nb ions, will preferentially form the tetragonal tungsten bronze structure instead of the expected orthorhombic structure [14]. This current work indicates that both of these arguments may be correct. Additions of vanadium pentoxide promotes the formation of tungsten bronze for SN and BN. However, the addition of vanadium pentoxide to SBN65 reduced the amount of the tungsten bronze phase that formed, similar to Neurgaonkar *et al.*'s observation that conversion of Nb^{+5} to Nb^{+4} inhibits the formation of the tungsten bronze phase for SBN. Addition of vanadium ions makes the tungsten bronze structure no longer stable for SBN65, most likely by changing the local coordination and arrangement of the oxygen octahedral.

3.2. Densification and microstructure

In this study, the applied sintering temperature of 1200°C is significantly lower than the sintering temperatures used in previous studies of bulk SBN [3, 5, 9]. Sintering time and temperature can be varied to achieve a desired grain size distribution and density. The density of the ceramics obtained from this solution chemistry approach are low (80–85% of the theoretical density) and did not significantly increased after 1 hour of sintering (Fig. 5). On the other hand, conventional techniques produce even lower densities (around 65% of the theoretical density) [3] when the ceramics are sintered around 1200°C.

V_2O_5 addition significantly increase the density of the ceramics except for SBN65 ceramics. The increase in the density is due to the increase in diffusion rates through a liquid phase (V_2O_5 melts at 690°C) along with the formation of the high-density tungsten bronze phase. For SBN65, addition of V_2O_5 increases the amount of an unknown phase with presumably a lower density.

The SEM micrograph obtained from the BN ceramic sintered for 1 hour at 1200°C show a nano–scale grain size, typical of the other SBN materials (Fig. 6). Grains grew uniformly as the sintering time increased. SBN ceramics sintered for 24 hours have a grain size between 1–5 μm. (Fig. 7). Microstructural analysis by SEM show that densification is likely hindered by the large agglomerate size (<36 μm) of the powders. The voids between the particles kept the maximum densification to around 80–85% of the theoretical density ($\rho_{SBN50} = 5.368$ g/cm^3).

It has been shown by previous researches that SBN is likely to show abnormal grain growth and has been difficult to densify [5]. Sintering temperatures higher than 1400°C result in a decrease in density due to abnormal grain growth [3] and a long sintering time causes the

development of duplex microstructure [9]. Introduction of a new fabrication method with high sintering rates at lower temperatures, such as solution chemistry approach, may be a major improvement in the quality of the SBN ceramics. The sintering rate of ceramics can be significantly affected by the homogeneity and the particle size of the ceramic powders. In the current work, there was no clear pattern observed in the sintering rates of solution derived ceramics with different Sr/Ba ratio (Fig. 6) and the rapid sintering throughout the solid solution may be due to excellent mixing of metal organics, at atomic level in the sols, resulting in excellent homogeneity in dried gels. Furthermore, the weak bonding between the metal atoms and organic groups allows metal oxide formation at very low temperatures under oxidizing conditions. Crystallization occurs between homogeneously distributed molecules without a need of long-range diffusion. Powders produced by solution chemistry processing possess excellent homogeneity and therefore, have the advantage of low temperature formation of crystalline SBN.

The liquid phase formed with the V_2O_5 addition drastically alters the microstructure of the sintered ceramics. The isotropic grains in SBN ceramics transform to rod like grains after the addition of V_2O_5 due to anisotropic grain growth (Fig. 8). Nishiwaki *et al*. [9], who produced similar results in SBN30 ceramics, found that grain elongation was along the *c*-axis, presumably due to preferential grain growth along this axis in the liquid phase. Our results show that grain elongation after V_2O_5 addition occurs throughout the $BaNb_2O_6$-$SrNb_2O_6$ system, although at different magnitudes. Grain elongation is less pronounced in $BaNb_2O_6$ compared to Sr containing compounds. There was no other significant difference in the grain morphology of the ceramics with different Sr/Ba ratio (Figs 7 and 8).

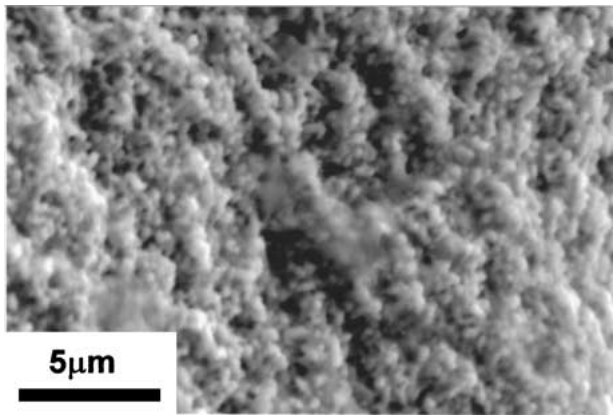

Figure 6 SEM micrograph of $BaNb_2O_6$ ceramic annealed at 1200°C for 1 hour.

3.3. Dielectric properties

In general, Sr rich solid solutions of SBN have a higher dielectric constant than Ba rich solid solutions due to the proximity of the Curie temperature to room temperature. In this current work, measured room temperature

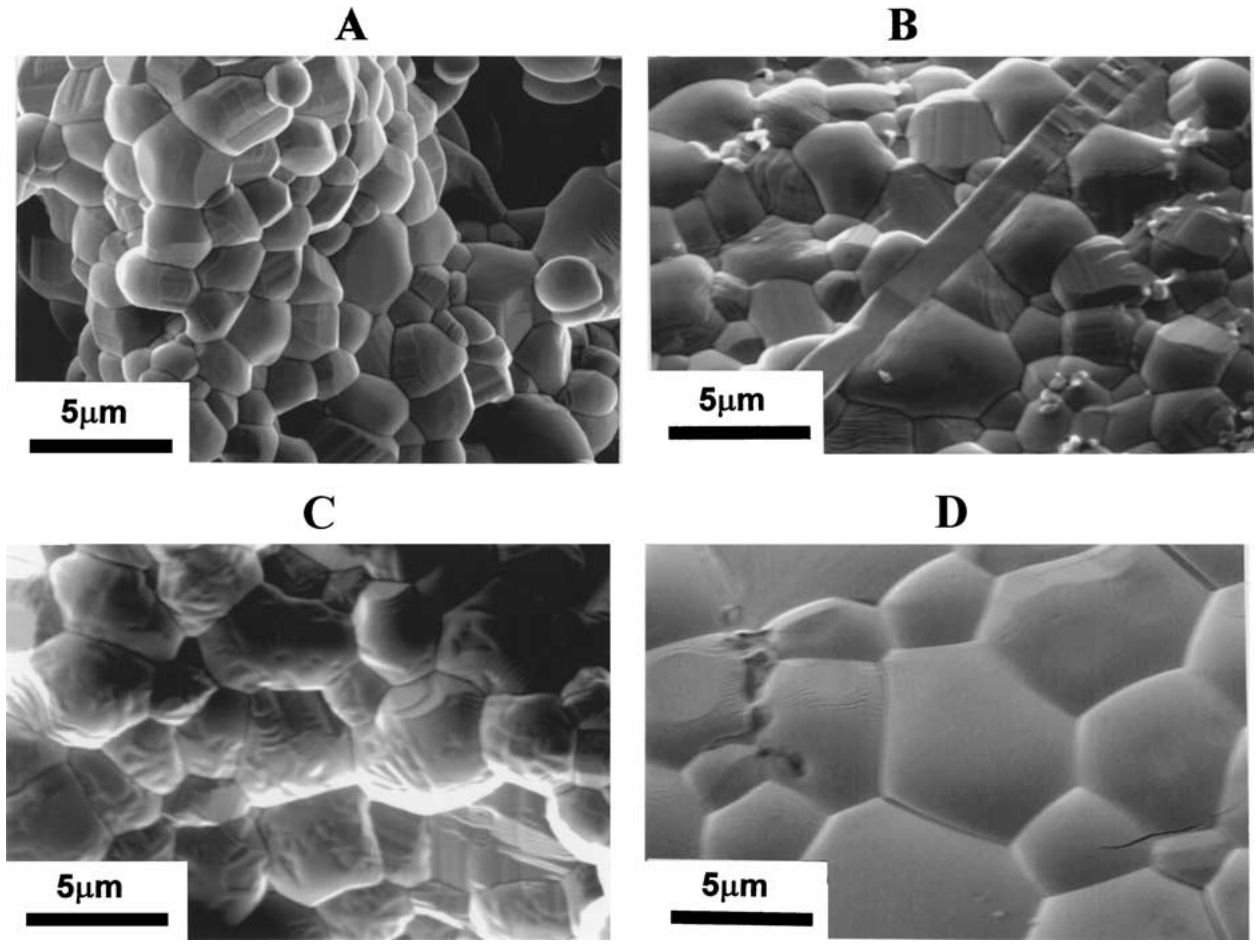

Figure 7 SEM micrographs of a) BN b) SBN30 c) SBN65 d) SN ceramics annealed at 1200°C for 24 hours.

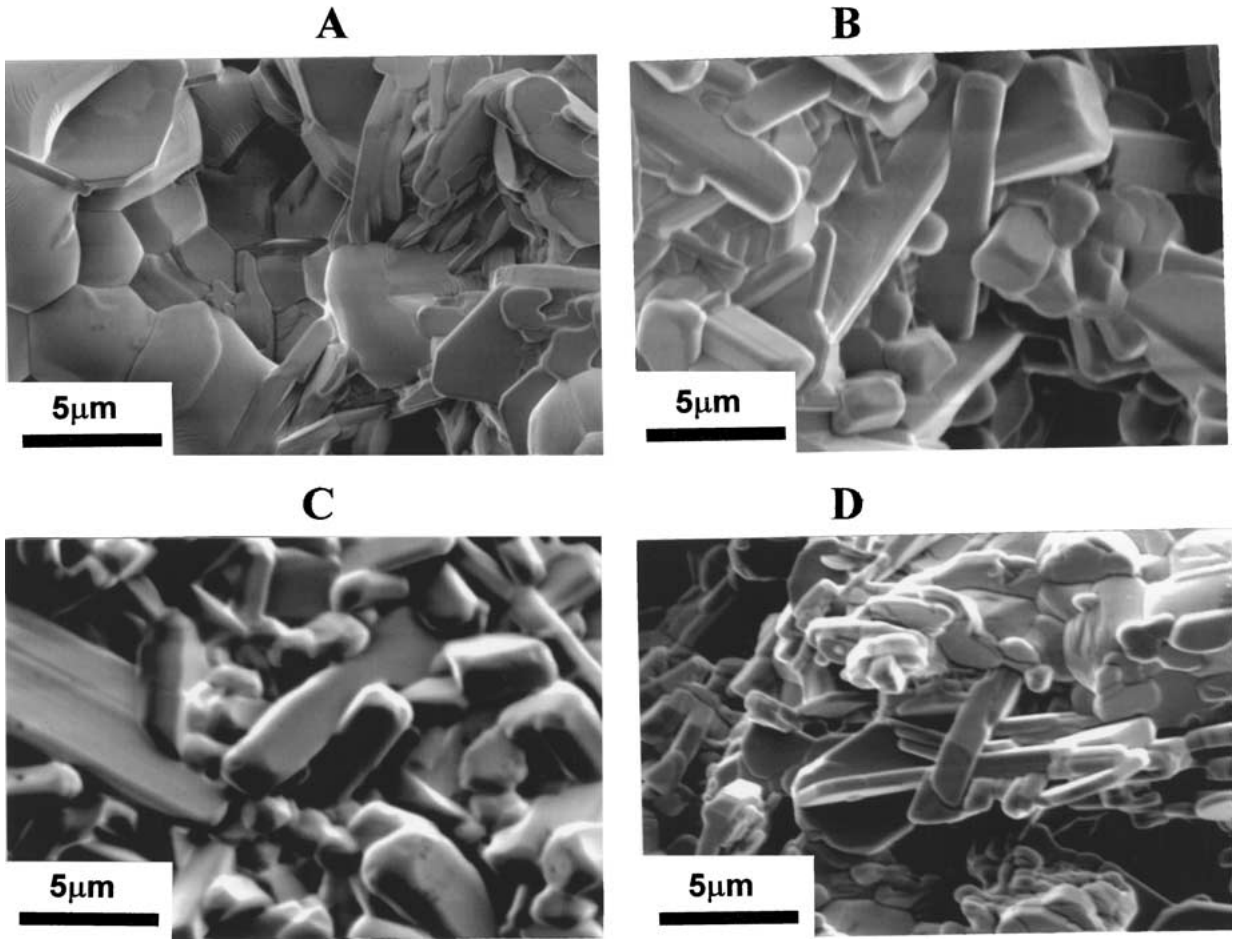

Figure 8 SEM micrographs of a) BN b) SBN30 c) SBN65 d) SN ceramics with 1% V_2O_5 addition annealed at 1200°C for 24 hours.

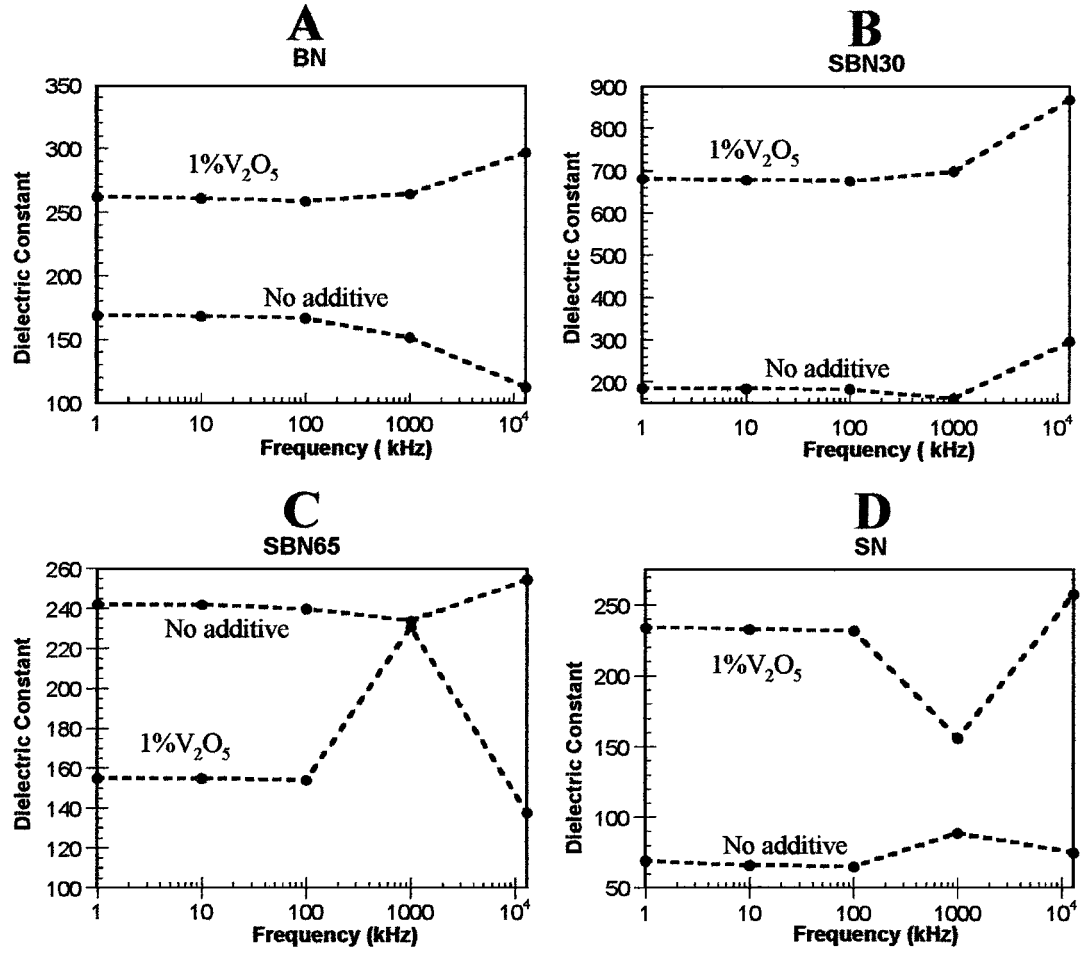

Figure 9 Frequency dependence of dielectric constant of ceramics with and without V_2O_5 addition. (a) BN; (b) SBN30; (c) SBN65; (d) SN.

dielectric constants of SBN ceramics (Fig. 9) are lower than the dielectric constants of higher density SBN ceramics fabricated at higher temperatures by the previous researchers. For example, VanDamme *et al*. [5] measured the room temperature dielectric constant of SBN65 ceramics to be 1700 at 1 kHz while the dielectric constant of the SBN65 ceramics in this work are 154 at 1 kHz (Fig. 9c). Nishiwaki *et al*. [9] observed that 1 wt% V_2O_5 additions to SBN30 ceramics decreases the dielectric constant from 600 to 240. In contrast, addition of 1 wt% V_2O_5 to SBN30 ceramics in this work increases the dielectric constant from 190 to 690 (Fig. 9b). The dielectric constant of the SBN ceramics do not show significant variations at different frequencies in the low frequency range but there are significant fluctuations at high frequencies (Fig. 9). The ceramics that consist predominantly of the tungsten bronze phase show the highest dielectric constants. V_2O_5 additions may increase the dielectric constant by both enhancing the formation of the tungsten bronze phase and increasing the density (Fig. 9). However, SBN65 ceramics show decreased values of dielectric constant with the V_2O_5 addition due to the presence of an unknown phase with a presumed low dielectric constant.

4. Conclusions

1. Low temperature ($<800^\circ$C) crystallization of BN, SBN, and SN powders was achieved by a solution chemistry approach, using alkoxides in acetic acid.

2. The tetragonal tungsten bronze structure was found present in all SBN compounds sintered at 1200°C from $x = 0$ to $x = 1$, including SN and BN.

3. The tungsten bronze phase in SBN65 obtained after the low temperature calcination was not stable at higher sintering temperatures in air and partially transformed to an unknown phase.

4. V_2O_5 additions enhanced the formation of the tungsten bronze phase for all compounds except SBN65. BN and SN ceramics primarily crystallized in a tetragonal tungsten bronze structure when 1 wt% V_2O_5 was added.

5. V_2O_5 additions increased the dielectric constant and density of SBN ceramics except for SBN65.

References

1. W. SAKAMOTO, T. YOGO, K. KIKUTA and S. HIRANO, *J. Amer. Ceram. Soc.* **79** (1996) 2283.
2. T. FANG and N. WU, *J. Mater. Sci.* **30** (1995) 3376.
3. W. LEE and T. FANG, *J. Amer. Ceram. Soc.* **81** (1998) 1019.
4. J. CARRUTHERS and M. GRASSO, *J. Electrochem. Soc.* **117** (1970) 1426.
5. N. VANDAMME, A. SUTHERLAND, I. JONES and S. WINZER, *J. Amer. Ceram. Soc.* **74** (1991) 1785.
6. D. SPINOLA, E. MOREIRA, L. BASSORA and D. GARCIA, The Proceedings of IEEE Ultrasonic Symposium, San Antonio, Texas, November 1996, edited by M. Levy, S. C. Schneider and B. R. Mcavoy (New York, 1996) p. 523.
7. S. DESHPANDE, H. POTDAR, P. GODBOLE and S. DATE, *J. Amer. Ceram. Soc.* **75** (1992) 2581.
8. W. LEE and T. FANG, *ibid.* **81** (1998) 300.
9. S. NISHIWAKI, J. TAKAHASHI and K. KODAIRA, *Jpn. J. Appl. Phys.* **33** (1994) 5477.
10. C. LUK, C. MAK and K. WONG, *Thin Solid Films* **298** (1997) 57.
11. A. Y. ORAL and M. L. MECARTNEY, *Ceramic Transactions* **95** (1999) 129.
12. T. FANG, N. WU and F. SHIAU, *J. Mater. Sci. Lett.* **13** (1994) 1746.
13. S. THONY, S. K. YOUDEN, J. HARRIS and L. HESSELINK, *Appl. Phys. Lett.* **65** (1994) 2018.
14. R. ROTH and J. WARING, *Journal of Research of the National Bureau of Standards-A. Physics and Chemistry* **65** (1961) 337.
15. A. BALLMAN and H. BROWN, *J. Cryst. Growth* **1** (1967) 311.
16. R. NEURGAONKAR, I. SANTHA and J. R. OLIVER, *Mater. Res. Bull.* **26** (1991) 983.

Received 24 November 1999
and accepted 16 July 2001